

On the Two Band Model in Pure and Doped BSCCO Superconductors

Ayman Al Sawalha¹

Abstract

The thermo-electric power S is calculated as a function of temperature for $\text{Bi}_2\text{Sr}_2\text{Ca}_{1-x}\text{Y}_x\text{Cu}_2\text{O}_{8+\delta}$ and $\text{Bi}_2\text{Sr}_2\text{Ca}_{2-x}\text{Sm}_x\text{Cu}_3\text{O}_{10}$ superconducting samples. This work is performed in terms of the reported data based on the considered samples; and with the help of the two band model. It is found that the measured values of S fit reasonably with the values which have been deduced from the model. The deduced parameters are used to calculate the energy gap E_g as a function of doping content and over a wide range of temperature. It is noteworthy that E_g is increased with increasing doping content and it is higher in Bi:2223 samples than Bi:2212. While E_g is decreased with decreasing temperature for pure samples; and vice versa for doped samples. On the other hand, the hole carrier concentration per Cu/ion is calculated by using the two-band Hubbard model and it is higher in Bi:2212 samples than Bi:2223. Our results are discussed in terms of both carrier concentration and hybridization for the two considered systems.

Keywords : band model , gap, superconductivity, BSCCO and carrier

Introduction

Since the discovery of high temperature superconductivity by Bednorz and Mullar [1], the aim of research in these materials has been directed toward their preparations and transport properties. The preparation is very important because we may obtain the room temperature critical temperature T_c during the substitution. While, the superconducting characterization attracted significant research interest for understanding the mechanism of superconductivity in these materials.

¹ Physics Department, Faculty of Science, Jerash University, Jerash, Jordan.

Seebeck coefficient is one of the transport properties complementary to the electrical resistivity and Hall effect. It is found that these properties are sensitive to the concentration of hole carriers in these materials. There exists an optimum concentration of holes at which the critical temperature T_c is maximum [2,3]. Below and above this concentration T_c decreases as a result of changes in carrier concentration, leading to dramatic changes in the transport properties. Therefore, a systematic study of transport properties and in particular thermopower is useful to understanding the role of hole carriers either in superconducting region or in metal-insulator transition region [4-7].

The thermoelectric power measurements S are primary performed to gain insight the nature of charge carriers responsible for the conduction process in the solid materials. It also provides an information about the bandwidths and the band gaps, which govern the transport properties of these materials [9,10]. Furthermore, the sensitivity of S depends on the energy dependence of the electron lifetime and the density of states near Fermi level. With the advent of high T_c superconductors, most of experimental and theoretical efforts have been directed towards the behavior of S in these materials [11,16]. The two-band model has been used early to explain that behavior [13,14]. Such a model has been successfully applied on pure and Pb substituted $\text{Bi}_{1.6}\text{Pb}_{0.4}\text{Sr}_2\text{Ca}_2\text{Cu}_3\text{O}_y$ sample [19-22].

In the present work, the thermo-electric power is calculated as a function of temperature for $\text{Bi}_2\text{Sr}_2\text{Ca}_{1-x}\text{Y}_x\text{Cu}_2\text{O}_{8+\delta}$ and $\text{Bi}_2\text{Sr}_2\text{Ca}_{2-x}\text{Sm}_x\text{Cu}_3\text{O}_{10}$ superconducting samples with various x values ($0.00 \leq x \leq 0.50$). This work is conducted in terms of reported data based on the above two considered BSCCO systems and with the help of the two band model. The fit between the measured and calculated values of S is made for all samples, and some fitting parameters are clearly evaluated. The energy gap is then calculated as a function of doping content and over a wide range of temperature for the considered samples. On the other hand, the carrier concentration per Cu/ion is also calculated by using the two-band Hubbard model and discussed for all samples.

Theory of Calculation

On the basis of refs. [17-19], the total S of Bi: 2223 system is given by;

$$S = -g\pi^2 \left\{ d \ln \sigma^+(E) / d \ln E \right\} T + 1/e \left\{ E_c + [k_B d \ln \tau(E) / d \ln E] T \right\} \exp(-\lambda / T), \quad (1)$$

where $\tau(E)$ is the relaxation time of electronic charge carriers of energy E , e is the electronic charge, k is the Boltzmann's constant, $\sigma^+(E)$ is the electrical conductivity, g is the number of Cu-O_2 planes in the superconducting system and λ is the parameter for a particular material, given by $(E_g/2k)$. Equation (1) is generally expressed as follows ;

$$S = A T + (B\lambda + C T) \exp(-\lambda / T), \quad (2)$$

where A , B , and C are the parameters for a particular material.

However, a typical formula could not be obtained when we fit the experimental data by using the exponential fit programme (Exam, DSC analysis version 1988). But we could obtain a formula which gave us the well fitting for the experimental values of S . Interestingly, we find that this formula will help us to calculate the energy gap over a wide range of the temperature concerned, which is not available by equation 2.

The best fit formula as follows ;

$$S = B^* + (A^* - B^*) \exp. \{(T - T_0) / P\}, \quad (3)$$

where A^* , B^* , T_0 and P are the best fit parameters. T_0 is the temperature representing the minimum of (dS/dT) against T . The calculated values of S deduced from the fitting can be plotted and compared with the measured values.

Since, equation 2 has been used early for calculating the values of S , we did analogies between equation (2) and equ. (3) as follows ;

$B^* = A T$, $A^* - B^* = B\lambda + C T$ and $\lambda = - \{T (T - T_0) / P\}$. The variation of B^* with doping is an indicator for the correlation between oxygen content and hole carriers in these systems [18]. By using the values of both T_0 and P , the values of λ are calculated over a wide range of the temperature concerned. In terms of the values of λ , the energy gap E_g can be easily calculated by using the following formula;

$$E_g = 0.8625 \times 10^{-4} \lambda \quad (\text{eV}) \quad (4)$$

To complete this scenario, the hole concentration per Cu ion at room temperature (H) is calculated by using the two-band Hubbard model. H can be expressed in terms of the thermoelectric power as follows [5,23,24];

$$S (\mu\text{V/K}) = k_B / e \{ \ln (1 - H / 2H) - \ln 2 \} \quad (5)$$

Model Application and Discussion

Figures 1 and 2 show the temperature dependence of S for $\text{Bi}_2\text{Sr}_2\text{Ca}_{1-x}\text{Y}_x\text{Cu}_2\text{O}_8$ and $\text{Bi}_{1.7}\text{Pb}_{0.3}\text{Sr}_2\text{Ca}_{2-x}\text{Sm}_x\text{Cu}_3\text{O}_{10}$ samples with various x values ($0.00 \leq x \leq 0.50$). The open triangles represent the experimental values of S as reported in refs. [5,8]; while the open squares represent the calculated values. The experimental points near T_c are shifted from the fitting. This is because the sharp drop in S near T_c is originated from the thermodynamic superconducting fluctuations [25]. It is found that the measured values of S fit reasonably with the values which have been deduced from the two-band model. S increases with decreasing temperature for all samples, then passes through a maximum and it falls sharply around T_c . The values of S are positive above T_c with $dS/dT < 0.00$ for the doped samples. While the values of S are negative for pure and $Y = 0.25$ samples. Also, S becomes negative at high temperatures ($T \geq 250$ K) for most of the considered samples. These results indicate that the hole carriers are responsible for the electric conduction in these samples similar to R: 123 superconductors. The change of S from positive to negative at high temperatures implies the presence of more than one type of charge carriers. This also suggests that the net S is the sum of contributions from the majority of hole carriers, which are thought to be responsible for superconductivity in these materials as well as electrons. The negative values of S for pure samples indicates that the electron carriers dominates the hole carriers. But the number of hole carriers still remains constant with the optimum value required for high T_c in these materials. This has been interpreted in terms of strong coulombs' interaction and correlation effects between carriers within the Hubbard Model [18, 26].

The best fit parameters A^* , B^* , T_0 and P for all samples are listed in Table (1). The behaviors of these parameters against doping content are also shown in Figure 3 (a-d). It is clear these parameters increase with increasing doping content and go to maximum at under doped region, followed by either decrease or increase at over doped region. It is well known that A^* is related to the contribution from the mobile holes in the Cu-O_2 planes; while B^* is an indicator about correlation between the oxygen content and hole carriers in these systems [18].

Therefore, the variation of these parameters with doping content indicates that oxygen content may be changes with the doping along with a decrease in the number of hole carriers. These results are in a good agreement with the reported data, which revealed that the rare-earth elements lead to a decrease in the hole carriers, thereby lowering the metallicity of the Bi-O layer [27].

Table 1 (a) : A^* , B^* , T_0 , T_c^{mf} , P , S_{250} , $E_g(0)$ and H Parameters at Different Values of Sm Content for Bi:2223 System

Y content	A^*	B^*	P	T_0 (K)	T_c^{mf} (K)	S (250 K)	$H / \text{Cu ion}$
0.00	- 5.012	0.683	107	233.6	85	-6.34	0.36
0.15	-0.25	69.40	1202	265.8	119	0.62	0.33
0.25	-4.73	0.52	99.6	226.8	77	-6.31	0.31
0.35	6.22	13.35	66.2	244.2	110	4.50	0.30

Table 1 (b) : A^* , B^* , T_0 , T_c^{mf} , P , S_{250} , $E_g(0)$ and H Parameters at Different Values of Sm Content for Bi:2223 System

Sm content	A^*	B^*	P	T_0 (K)	T_c^{mf} (K)	S (250 K)	$H / \text{Cu ion}$
0.00	- 5.012	-3.18	46	123	117	-2.60	0.35
0.10	5.30	102	1358	221	91	2.57	0.33
0.20	1.63	37.15	221.3	293	90	6.11	0.32
0.50	17.76	36.5	109	255	88	16..80	0.29

Figure 4 (a,b) shows the variation of E_g as a function of temperature and different values of doping content for all samples, respectively. The behavior of E_g are summarized as follows :

- 1- E_g is zero for all samples at T ($T = T_0$), in which (dS/dT) versus temperature is minimum.
- 2- E_g is positive at T ($T > T_0$) , and it becomes negative at T ($T < T_0$) for pure samples. While E_g is negative at T ($T > T_0$) , and it becomes positive at T ($T < T_0$) for doped samples.
- 3- E_g is nearly negative for pure samples. It becomes nearly zero at low doping content , and goes to positive values with further increase of doping content.

- 4- E_g is higher for Bi:2223 samples as compared to Bi:2212 { $E_g = (-0.15 - 10 \text{ meV})$ for Bi: 2212 ; and { $E_g = (-1.5 - 75 \text{ meV})$ for Bi 2223}.
- 5- E_g is directly proportional with the temperature for pure samples, and vice versa for the doped samples.
- 6- The lower values of E_g is generally occurred at $T = T_c^{mf}$ for pure samples and vice versa for the doped samples. T_c^{mf} is the mean field temperature, estimated from the maximum of (dS/dT) versus temperature.

It is interesting to mention here that the behavior of E_g is totally different for Bi:2212 samples than Bi:2223. Also, E_g is different for pure samples than the doped samples. The higher values of E_g for Bi:2223 samples as compared to Bi:2212 may be caused by the strongest of 3d-2p hybridization in the Bi:2223 system as compared to Bi:2212. However, it has been reported that the weakness in the hybridization of high T_c materials eventually causes reduction of the bandwidth, and consequently the energy gap was decreased [28,29]. The increase of E_g with doping is attributed by decreasing the number of hole carriers produced by the doping. This is in good agreement with previous work which indicate that the presence of doping in the superconducting material lead to the mixing of s and d electrons [30,31]. Therefore, the Cooper pair will be formed by the hybridized quasi-particles which have both s and d electron properties.

To complete this scenario, E_g is calculated at 0 K by using BCS formula, $E_g(0) = 3.2 k_B T_c$. The values of $E_g(0)$ are listed in Table 1. These values are ranges between (21-33 meV) for Bi:2212 system, and (24-32 meV) for Bi:2223 system. For comparison between these values and with those calculated by using the present model, we have calculated E_g at T_c^{mf} values listed in Table 1. We would like to mention here that T_c^{mf} is the lowest temperature available for us since the fit parameters are calculated at that temperature. The different values of E_g at the considered temperatures are listed in Table 2. It is clear that the values of $E_g(0)$ are higher than $E_g(T_c^{mf})$. This behavior indicates that E_g was increased as one moves towards lower temperature (0 K). This is due to increasing the width of the conduction band or due to band broadening with decreasing temperature, which results in shifting the Fermi energy level from its original position to the edge of the band or to a position located near the boundary of localized states [32].

Table 2 : E_g Versus Y and Sm Contents for Bi:2212 and Bi:2223 Systems

Y content	$E_g(0)$ (meV)	$E_g(T_c^{mf})$ (meV)	Sm content	$E_g(0)$ (meV)	$E_g(T_c^{mf})$ (meV)
0.00	23	10	0.00	32	1
0.15	33	3	0.10	25	10
0.25	21	10	0.20	25	10
0.35	30	20	0.50	24	12

Finally, the hole carrier concentration per Cu ion H is calculated as a function of doping content and shown in Figure 4 (c). It is noted that H is decreased by the doping and almost linearly for the two considered systems. Further, the values of H are higher in Bi:2212 samples than Bi:2223. The decrease of H with doping is due to substitution by R^{3+} at Ca^{2+} sites. While, the higher values of H in Bi:2212 than Bi:2223 are consistent with E_g behavior. However, thermoelectric power for the Y-doped Bi:2212 system has been investigated as a function of temperature and at different values of doping content. It has been found that the substitution of Y^{3+} for Ca^{2+} decreasing the hole concentration than its optimum value required for high T_c [5, 33, 34]. Furthermore, Wang et.al. have been found a shift of S toward more positive values in post annealed R^{3+} substituted at Ca^{2+} in Bi:2223 systems [35] ($R = Sm^{3+}, Gd^{3+}$). They explained this behavior as a result of decreasing the hole concentration as well as in the considered samples. These results indicate that the reduction of hole carriers makes a positive contribution to hybridization, and consequently the energy gap was increased. Anyhow, Further work is necessary to reveal the E_g behavior and its actual mechanism in superconductivity.

Conclusion

By using two band model, the thermo-electric power S is calculated for $Bi_2Sr_2Ca_{1-x}Y_xCu_2O_{8+\delta}$ and $Bi_2Sr_2Ca_{2-x}Sm_xCu_3O_{10}$ superconducting samples. We have shown that the measured values of S fit reasonably with the values which have been deduced from the two band model. The fitting parameters are well used for calculating the energy gap E_g as a function of doping content and over a wide range of temperature. It is found that E_g is increased with increasing doping content and it is higher in Bi:2223 samples than Bi:2212. Furthermore, E_g is increased with increasing temperature for pure samples and vice versa for doped samples.

We believe that both carrier concentration and hybridization are playing a major contribution for the energy gap of the two considered systems. Further work is necessary to reveal the E_g behavior and its actual mechanism in superconductivity.

Acknowledgments

The authors would like to thank the Deanship of Scientific Research, King Faisal University for maintenance support during the present work.

References

- J.G. Bednorz and K.A. Müller, Z.Phys. B64, 189 (1986).
 J.B. Torrance, Y. Tokura, A.I. Nazzari, A. Bezingue, T.C. Huang and S.S.P. Parkin, Phys. Rev. Lett. 61,1127 (1988).
 Y. Tokura, J.B. Torrance, T.C. Huang and A.I. Nazzari, Phys. Rev. B 38,7156 (1988).
 M.M. Ibrahim, S.M. Khalil, Eur. Phys. J.Appl. 14, 79 (2001).
 K.N. Kishore, S. satyavathi, M. Muralidhar, O. Pena, V.H. Babu, Physica C 252, 49 (1995).
 J.L. Cohn, S.A. Wolf, V. Selvamanickam, K. Salama, Phys.Rev. Lett. 66, 1098 (1991).
 A.E. Koshelev, G. Yu Logvenov, V.A. Larkin, V.V. Ryazanov, K. Ya Soifer, Physica C 177, 129 (1991).
 S.M. Khalil, J. Phys.Chem. of Solids 64, 855(2003).
 D. K.C. MacDonald, Thermoelectricity: An Introduction to the Principles (Wiley, New York, 1962).
 I. M. Tsidilkovski and V. I. Tsidilkovski, Solid State Commun. 66, 51 (1988).
 C. Uher and A.B. Kaiser, In Studies of High Temperature Superconductors, Edited by A. Narlikar (Nova Science, New York, 7, 352 (1992).
 P. W. Anderson, G. Bhaskaran, Z. Zhou, J. Wheatley, T. Hsu, B.S. Shastry, B. Doucot and S. Liang, Physica C 153-155, 527 (1988).
 M.M. Ibrahim, S.M. Khalil, Eur. Phys. J. Appl. 14, 79 (2001).
 Mehmet Ali Aksan and Mehmet Eyyuphan Yakinci, J. Alloys and Compounds 385,33 (2004).
 M. Matusiak, T. Plackowski and C. Sulkowski, Physica C 387, 183 (2003).
 M.M. Ibrahim, S.M. Khalil and A.M. Ahmed, J. Phys.& Chem. of Solids 61, 1553 (2000).
 C. Uher and A.B. Kaiser, Phys. Rev. B 36, 5680 (1987).
 Y. Xin, K. W. Wang, C.X. Fan, Z. Z. Sheng and F. T. Chang, Phys. Rev. B 48, 557 (1993).
 V.P.S. Awana, V. N. Moorthy and A.V. Narlikar, Phys. Rev. B 49, 9, 6385 (1994).
 G.G.Qian, K.Q. Ruan, X. H. Chen, C.Y. Wang, L. Z. Cao and M.R. Ji, Physica C 313, 58 (1999).
 M. Chandra Sekhar, S.V. Suryanarayana, Physica C 415, 209 (2004).
 A.Sedky and A.A. Ahmed, Chinese J. of Physics 41,5,511 (2003).
 P. Mandal, A. Poddar, B. Ghosh and P. Choudhury, Phys. Rev. B 43, 16, 13102 (1991).
 J. B. Mandal, S. Keshri, P. Mandal, A. Poddar, A. N. Das and B. Ghosh, Phys. Rev. B 46, 11840 (1992).
 L. Forro, C. Kendziora and L. Mihaly, Phys. Rev. B 44, 2418 (1991).
 Marks. Hybertsen and L. F. Mattheiss, Phys. Rev. Letters 60, 16, 1661 (1988).
 S.B. Samanta, P.K. Dutta, V.P.S. Awana, E. Gmelin and A.V. Narlikar, Physica C 178, 171 (1991).

- A.Sedky,Abdalaziz A.Almulhem and Sobhy S. Ibrahim,submitted to Physica C .
 E.M. El-Maghraby, A.Sedky and A.Yehia, J.Low Temperature Phys. 133, 516, 387(2003).
 P.W. Anderson, J.Phys.Chem. Solids 11, 26 (1959).
 S. Punpocha, R. Hoonsawat and I.M. Tang, Solid State Comm. 129, 151 (2004).
 S. Neeleshwar, M. Muralidhar, M. Murakami and P. Venugopal Reddy, Physica C 391, 131 (2003).
 C.N.R. Rao, T.V. Ramakrishann and N. Kumar, Physica C 165, 183 (1990).
 F. Munakata, K. Matsuura, K. Kubo, T. Kawano and H. Yamauchi, Phys. Rev. B 45, 10604 (1992).
 J. Wang, M. Wakata, T. Kaneko, S. Takano and H. Yamauchi, Physica C 208, 323 (1993).

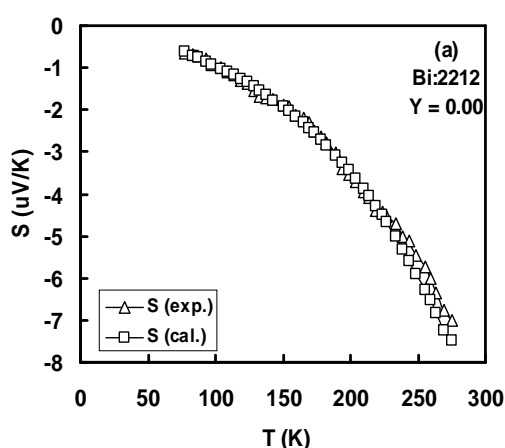


Figure 1 (A): Calculated and Measured Values of S Versus Temperature for Y Doped Bi:2212 Samples ($Y = 0.00$)

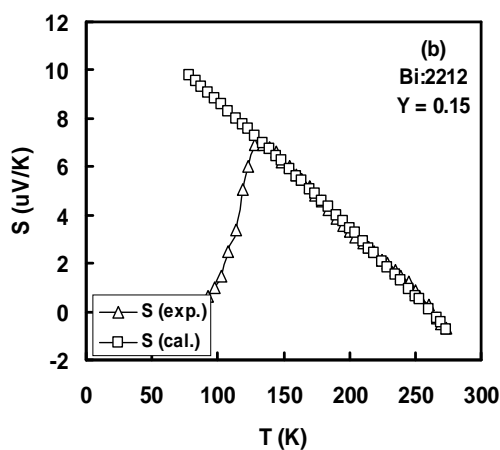


Figure 1 (b): Calculated and Measured Values of S Versus Temperature for Y Doped Bi:2212 Samples ($Y = 0.15$).

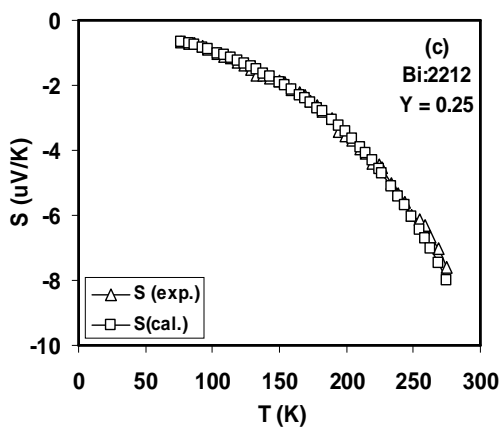


Figure 1 (c): Calculated and Measured Values of S Versus Temperature for Y Doped Bi:2212 Samples ($Y = 0.25$).

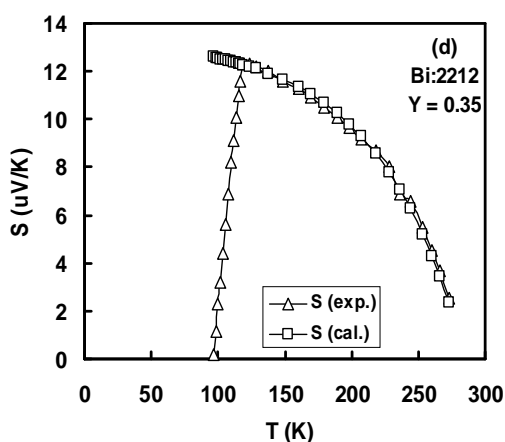


Figure 1 (d): Calculated and Measured Values of S Versus Temperature for Y doped Bi:2212 Samples ($Y = 0.35$)

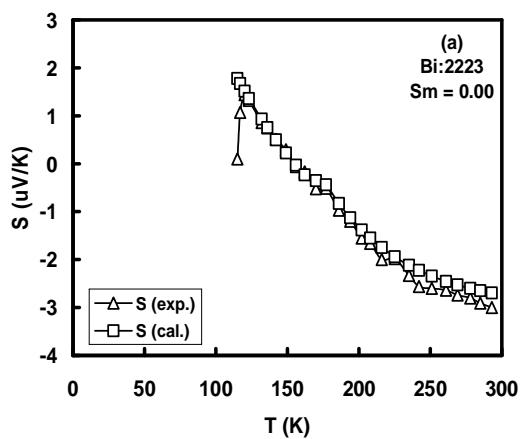


Figure 2 (a): Calculated and Measured Values of S versus Temperature for Sm doped Bi:2223 Samples ($Sm = 0.00$)

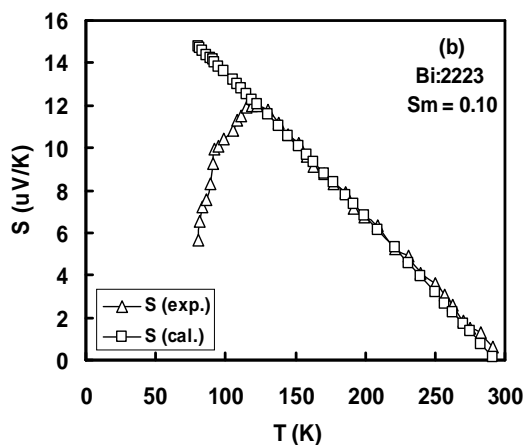
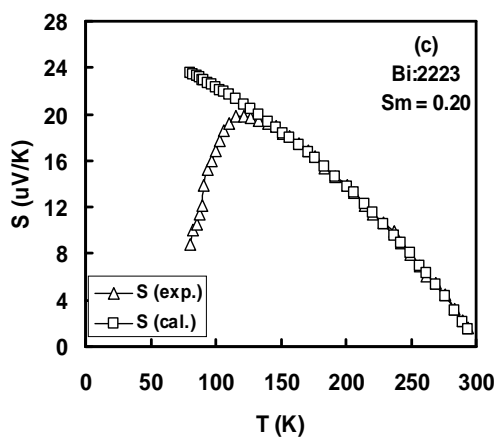


Figure 2 (b): Calculated and Measured Values of S Versus Temperature for Sm Doped Bi:22



23 Samples (Sm = 0.10).

Figure 2 (c): Calculated and Measured values of S Versus Temperature for Sm Doped Bi:2223 Samples (Sm = 0.20)

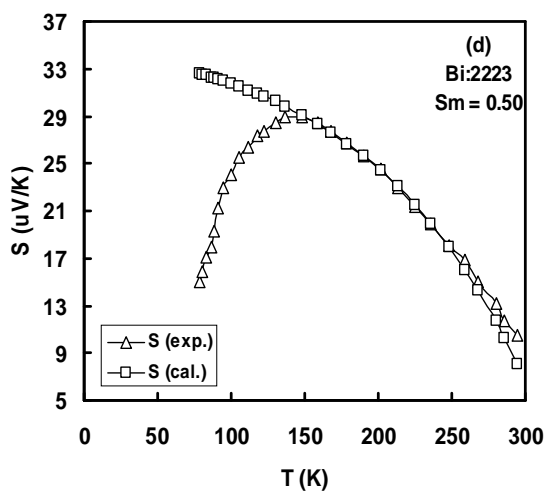


Figure 2 (d): Calculated and Measured Values of S Versus Temperature for Sm Doped Bi:2223 Samples ($Sm = 0.50$)

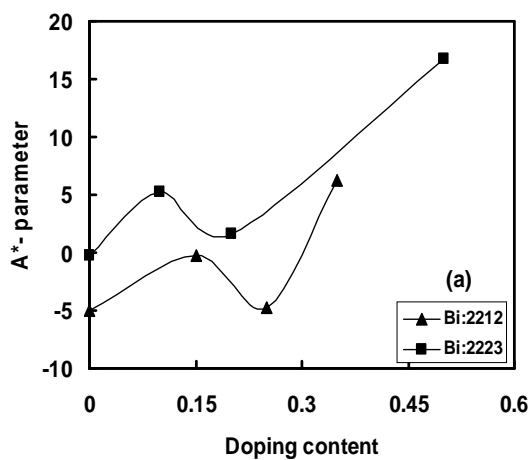


Figure 3 (a): A^* Versus Doping Content for Y Doped Bi:2212 and Sm Doped Bi:2223 Samples

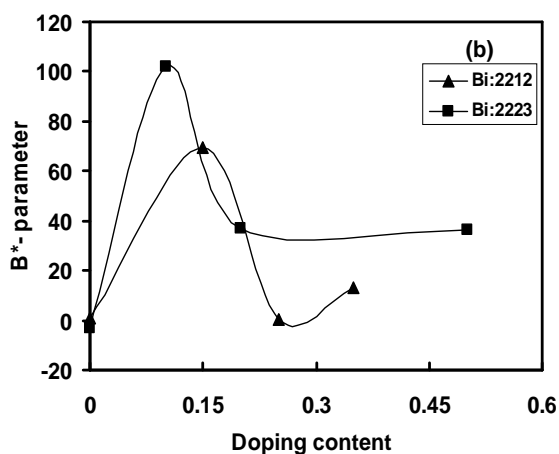


Figure 3 (b): B^* Versus Doping Content for Y Doped Bi:2212 and Sm doped Bi:2223 Samples

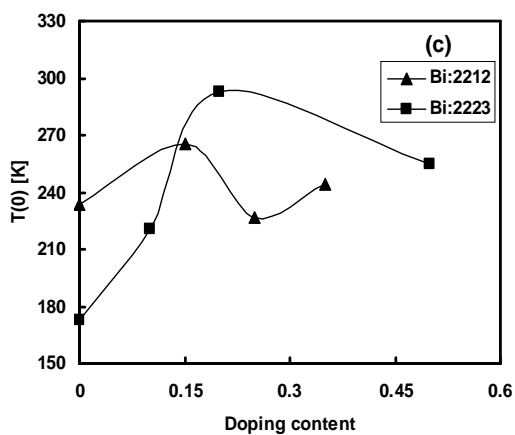


Figure 3 (c): T_0 Versus Doping Content for Y Doped Bi:2212 and Sm Doped Bi:2223 Samples.

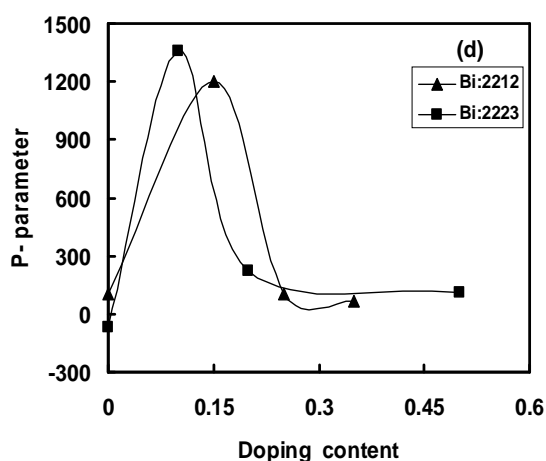


Figure 3 (d): P Versus Doping Content for Y doped Bi:2212 and Sm Doped Bi:2223 Samples

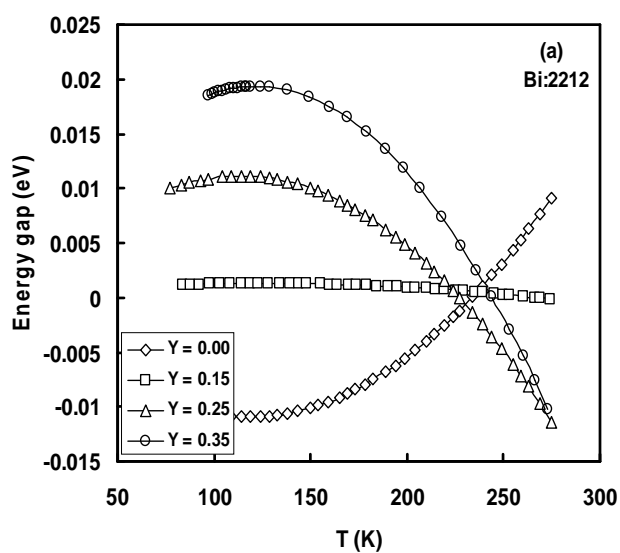


Figure 4 (a): E_g Versus Temperature at Different Values of Y Content for Bi:2212 Samples

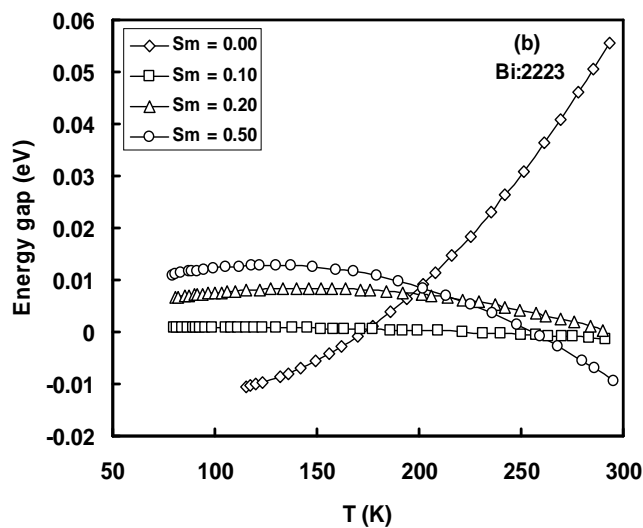


Figure 4 (b): E_g Versus Temperature at Different values of Sm Content for Bi:2223 Samples.

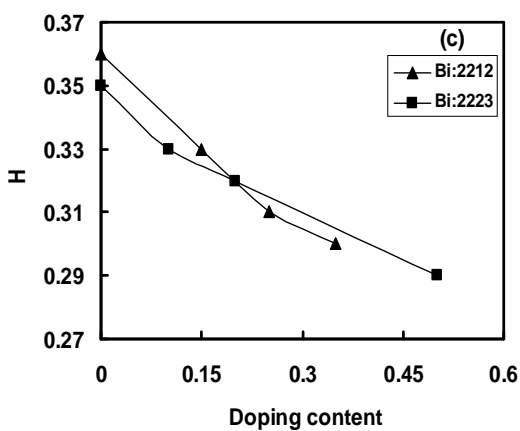


Figure 4 (c): H versus Doping Content for Y Doped Bi:2212 and Sm Doped Bi:2223 Samples